Supporting Information for:

Systematic comparison of vesicular targeting signals leads to the development of genetically-encoded vesicular fluorescent Zn^{2+} and pH sensors

Evan P.S. Pratt, Kelsie J. Anson#, Justin K. Tapper#, David M. Simpson, Amy E. Palmer*
Department of Biochemistry and BioFrontiers Institute
University of Colorado Boulder
3415 Colorado Ave, UCB 596
Boulder, CO 80309

# These authors contributed equally to this work

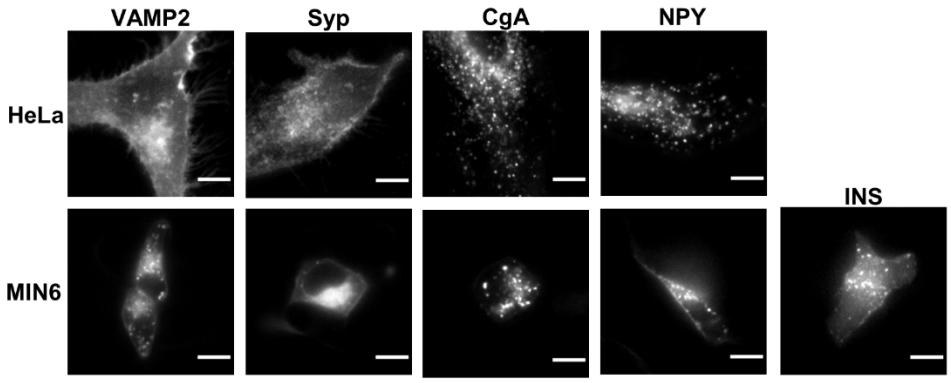

Figure S-1: Wide field fluorescence images of HeLa cells and MIN6 cells expressing secretory targeting domains fused with a fluorescent protein. Representative images of HeLa cells (top row) and MIN6 cells (bottom row) expressing VAMP2-mCherry, Syp-mCherry, CgA-mCherry, NPY-Cherry and INS-mCherry (MIN6 only) that were collected using a wide field confocal microscope. Scale bar = 10 μm.

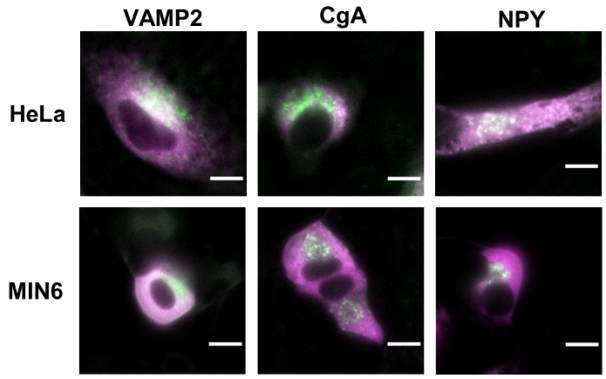

Figure S-2: Wide field fluorescence images of HeLa cells and MIN6 cells expressing secretory targeting domains fused with ZapCY1. Representative images of HeLa cells (top row) and MIN6 cells (bottom row) expressing VAMP2-ZapCY1, CgA-ZapCY1 and NPY-ZapCY1 that were collected using a wide field fluorescence microscope. The images shown are an overlay of the CFP channel (green) and YFP channel (magenta). Scale bar = 10 μm.

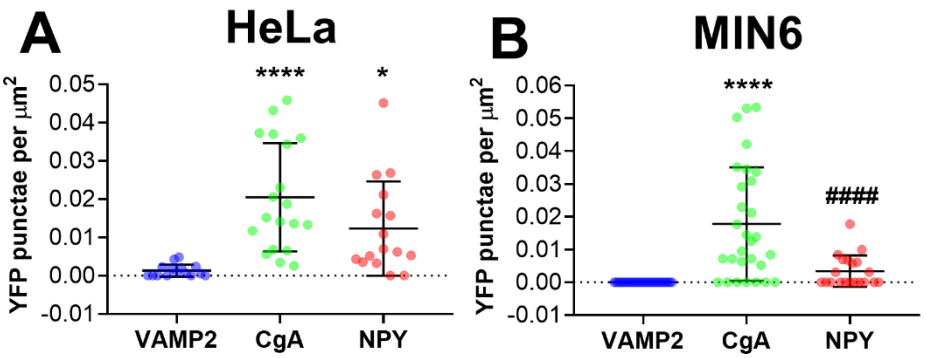

Figure S-3: Quantification of YFP puncta in cells expressing secretory targeting domains fused with ZapCY1. HeLa and MIN6 cells were transfected with VAMP2-ZapCY1, CgA-ZapCY1 and NPY-ZapCY1 and images were collected using a spinning disk confocal microscope. (A) Dot plot of YFP puncta detected per HeLa cell, normalized to surface area (μm^2). Three independent experiments were performed per construct, and the average ± standard deviation is shown for n= 15 cells (VAMP2), n=19 cells (CgA) and n=16 cells (NPY). Two outliers were identified in the VAMP2 group using the ROUT method (Q=1%) and removed from further analysis. Statistical analysis was performed using a One-Way ANOVA test with *post hoc* Tukey (****, $P < 0.0001$, *, $P < 0.05$ compared with VAMP2). (B) Dot plot of YFP puncta detected per MIN6 cell, normalized to surface area (μm^2). Three independent experiments were performed per construct, and the average ± standard deviation is shown for n=26 cells (VAMP2), n=29 cells (CgA) and n=20 cells (NPY). Using the ROUT method (Q=1%), two outliers were identified in the CgA group and three outliers were identified in the NPY group, and all outliers were removed from further analysis. Statistical analysis was performed using a One-Way ANOVA test with *post hoc* Tukey (****, $P < 0.0001$ compared with VAMP2; ####, $P < 0.0001$ compared with CgA).

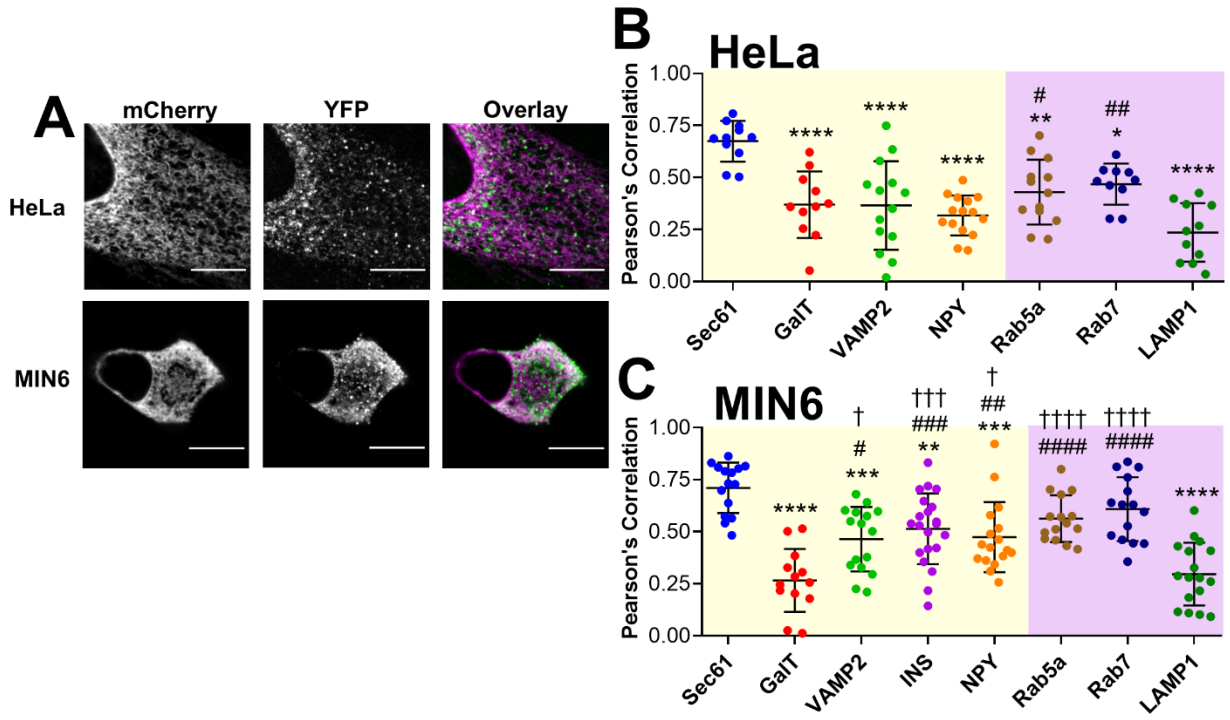

Figure S-4: Colocalization analysis of CgA-ZapCY1 (YFP signal) and fluorescent organelle markers in HeLa cells and MIN6 cells. (A) Representative image of HeLa cell (top) and MIN6 cell (bottom) coexpressing CgA-ZapCY1 and Sec61-mCherry that was collected using a spinning disk confocal microscope. Images collected in the mCherry channel and YFP channel are shown in greyscale, and an overlay of both images is shown in color (mCherry = magenta, YFP = green). Scale bar = 10 µm. (B&C) Dot plot of PCC values between YFP and mCherry calculated in HeLa cells (B) and MIN6 cells (C). mCherry markers of compartments in the secretory pathway and endo-lysosomal pathway are shaded in yellow and purple, respectively. In panel B, three independent experiments were performed per mCherry marker, and the average ± standard deviation is shown for n=11 cells (Sec61), n=11 cells (GalT), n=14 cells (VAMP2), n=15 cells (NPY), n=13 cells (Rab5a), n=10 cells (Rab7) and n=11 cells (LAMP1). Statistical analysis was performed using a One-Way ANOVA test with *post hoc* Tukey (****, P < 0.0001, **, P < 0.01, *, P < 0.05 compared with Sec61; ##, P < 0.01, #, P < 0.05 compared with LAMP1). In panel C, three independent experiments were performed per mCherry marker, and the average ± standard deviation is shown for n=15 cells (Sec61), n=13 cells (GalT), n=16 cells (VAMP2), n=21 cells (INS), n=17 cells (NPY), n=15 cells (Rab5a), n=15 cells (Rab7) and n=17 cells (LAMP1). Statistical analysis was performed using a One-Way ANOVA test with *post hoc* Tukey (****, P < 0.0001, ***, P < 0.001, **, P < 0.01 compared with Sec61; ####, P < 0.0001, ###, P < 0.001, ##, P < 0.01, #, P < 0.05 compared with GalT; ††††, P < 0.0001, †††, P < 0.001, †, P < 0.05 compared with LAMP1).

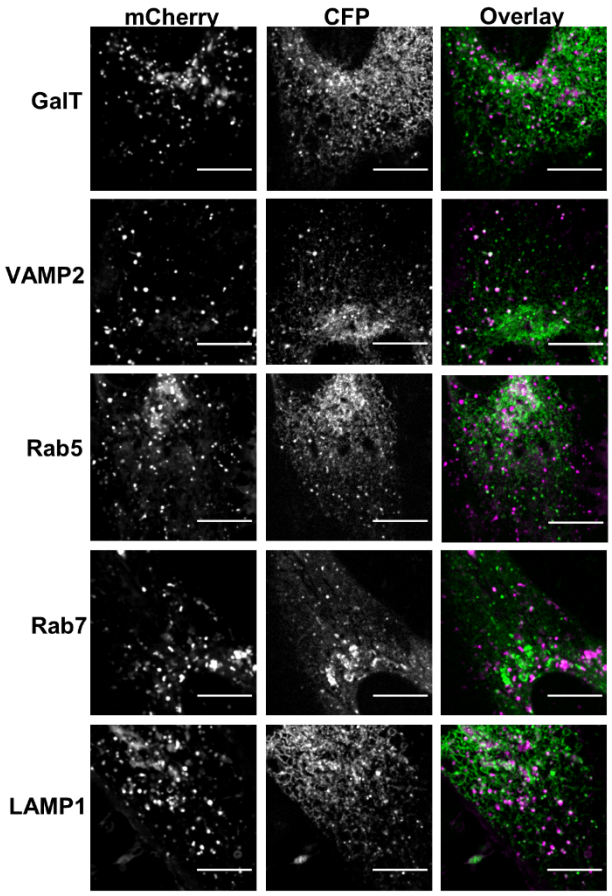

Figure S-5: Spinning disk confocal images of HeLa cells coexpressing CgA-ZapCY1 and fluorescent organelle markers. Representative images of HeLa cells coexpressing CgA-ZapCY1 and GalT-mCherry, VAMP2-mCherry, Rab5a-mCherry, Rab7-mCherry or LAMP1-mCherry. Images were collected using a spinning disk confocal microscope. Images collected in the mCherry channel and CFP channel are shown in greyscale, and an overlay of both images are shown in color (mCherry = magenta, CFP = green). Scale bar = 10 μm.

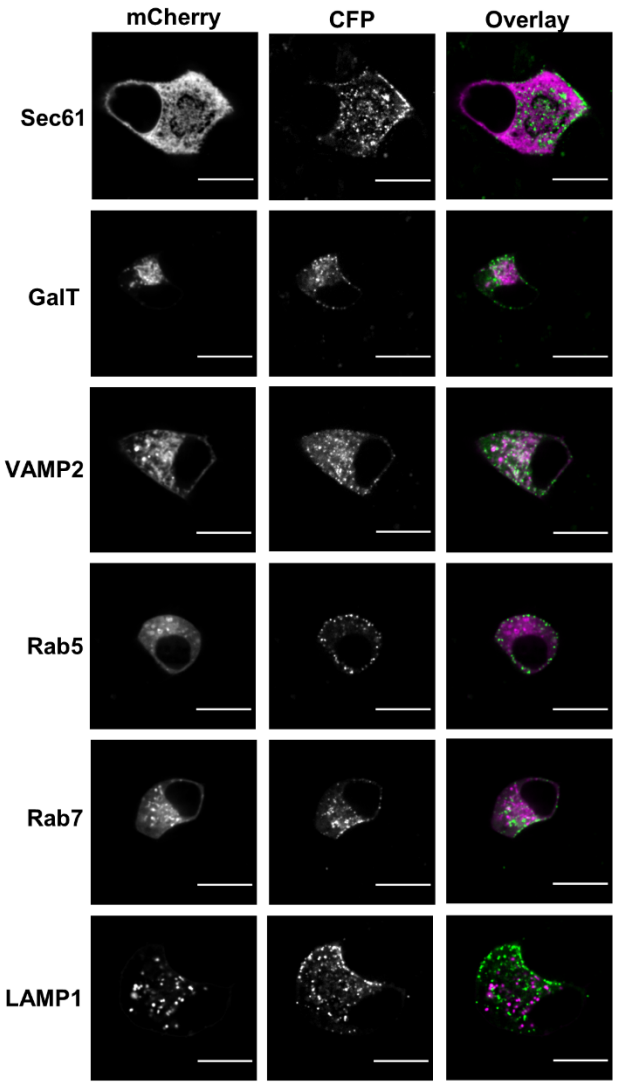

Figure S-6: Spinning disk confocal images of MIN6 cells coexpressing CgA-ZapCY1 and fluorescent organelle markers. MIN6 cells were cotransfected with CgA-ZapCY1 and Sec61-mCherry, GalT-mCherry, VAMP2-mCherry, Rab5a-mCherry, Rab7-mCherry or LAMP1-mCherry, and images were collected using a spinning disk confocal microscope. Images collected in the mCherry channel and CFP channel are shown in greyscale, and an overlay of both images are shown in color (mCherry = magenta, CFP = green). Scale bar = 10 μm.

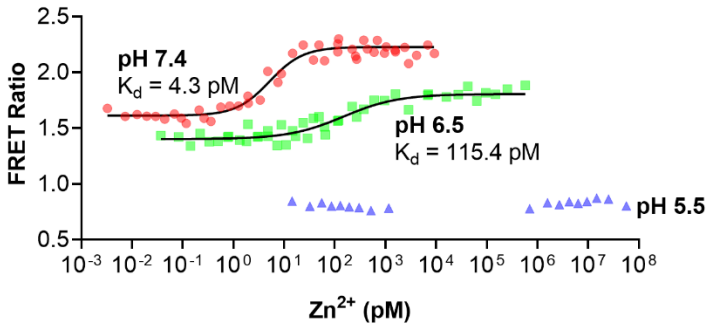

Figure S-7: Acidic pH affects the FRET ratio and Zn^{2+} binding affinity of purified ZapCY1 *in vitro*. *In vitro* titration of the FRET ratio of purified ZapCY1 across a range of free Zn^{2+} concentrations. Zn^{2+} titrations were performed using buffered Zn^{2+} solutions and in solutions buffered at three different pH (pH 7.4, pH 6.5 and pH 5.5).

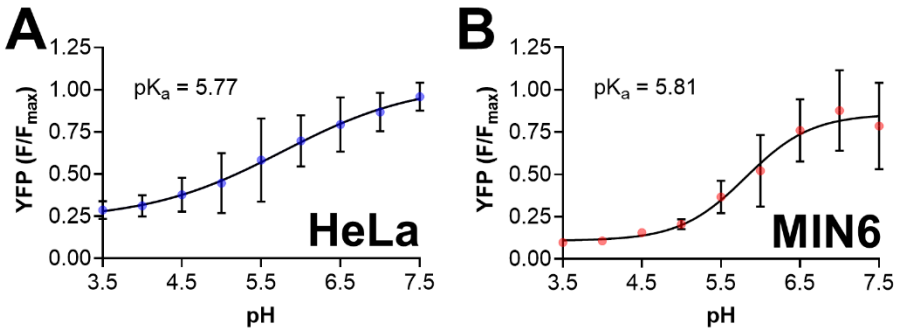

Figure S-8: pH titration of the YFP signal in individual vesicles expressing CgA-ZapCY1. HeLa and MIN6 cells expressing CgA-ZapCY1 were imaged using a spinning disk confocal microscope. (A) Titration of the YFP signal in individual secretory vesicles expressing CgA-ZapCY1 in HeLa cells across a range of pH values (pH 3.5-7.5). In each experiment, the YFP signal at every pH was normalized to the maximum YFP signal (F_{max}) to yield the normalized YFP signal (F/F_{max}). Four independent experiments were performed in HeLa cells, and the average ± standard deviation is shown for n=89 vesicles (pH 7.5), n=78 vesicles (pH 7), n=53 vesicles (pH 6.5), n=34 vesicles (pH 6), n=40 vesicles (pH 5.5), n=41 vesicles (pH 5), n=30 vesicles (pH 4.5), n=26 vesicles (pH 4) and n=28 vesicles (pH 3.5). Data points were fit with a four-parameter logistic regression curve to determine the pK_a. (B) Titration of the YFP signal in individual secretory vesicles expressing CgA-ZapCY1 in MIN6 cells across a range of pH values (pH 3.5-7.5). Four independent experiments were performed, and the average ± standard deviation is shown for=136 vesicles (pH 7.5), n=105 vesicles (pH 7), n=132 vesicles (pH 6.5), n=138 vesicles (pH 6), n=122 vesicles (pH 5.5), n=125 vesicles (pH 5), n=119 vesicles (pH 4.5), n=146 vesicles (pH 4) and n=133 vesicles (pH 3.5).

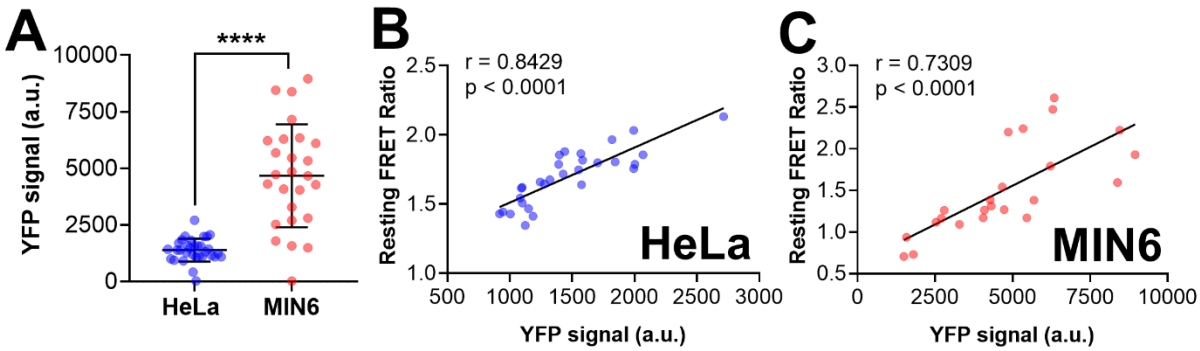

Figure S-9: Positive correlation between the resting FRET ratio and raw YFP signal. HeLa and MIN6 cells expressing CgA-ZapCY1 were imaged using a spinning disk confocal microscope, and individual vesicles were identified and tracked over the course of each experiment. (A) Dot plot of the YFP signal among secretory vesicles in HeLa cells (n=29 vesicles) and MIN6 cells (n=23 vesicles). One outlier was identified in the MIN6 group using the ROUT method (Q=1%) and removed from further analysis. Statistical analysis was performed using an unpaired t-test (****, P < 0.0001). (B) Scatter plot demonstrating the relationship between resting FRET ratio and YFP signal (n=29 vesicles). Points were fit with linear regression, and the Pearson correlation coefficient (r) was used to determine whether a correlation exists ($p < 0.05$ is considered significant). (C) Scatter plot demonstrating the relationship between resting FRET ratio and YFP signal in MIN6 cells (n=23 vesicles).

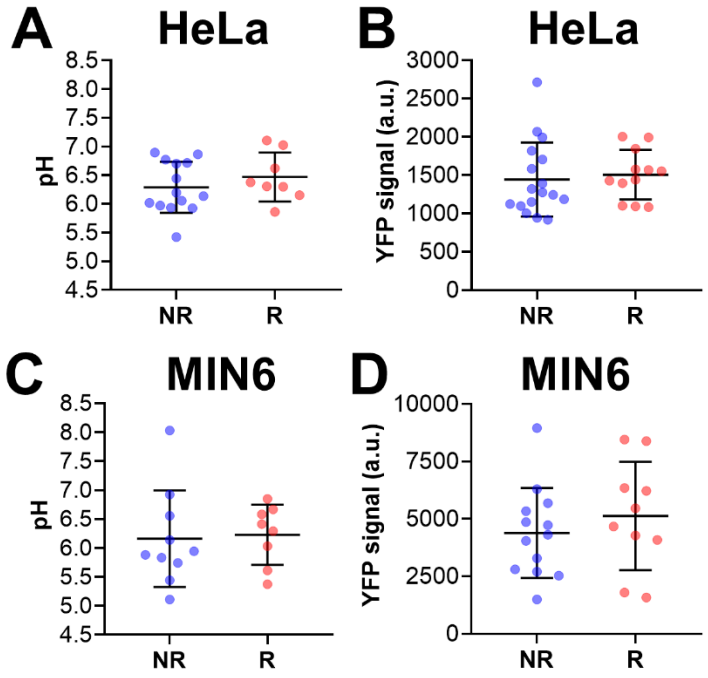

Figure S-10: Differences in Zn^{2+} response cannot be explained by pH levels or raw YFP signal. HeLa and MIN6 cells expressing CgA-ZapCY1 were imaged using a spinning disk confocal microscope, and individual vesicles were identified and tracked over the course of each experiment. Secretory vesicles were broken into two groups depending on their response to Zn^{2+} perturbations: non-responders (NR) or responders (R). (A) Dot plot of resting pH levels in secretory vesicles in HeLa cells: NR (n = 14 vesicles) and R (n = 8 vesicles). (B) Dot plot of the raw YFP signal in secretory vesicles in HeLa cells: NR (n = 17 vesicles) and R (n = 12 vesicles). (C) Dot plot of resting pH levels in secretory vesicles in MIN6 cells: NR (n = 10 vesicles) and R (n = 8 vesicles). (D) Dot plot of the raw YFP signal in secretory vesicles in MIN6 cells: NR (n = 13 vesicles) and R (n = 10 vesicles).

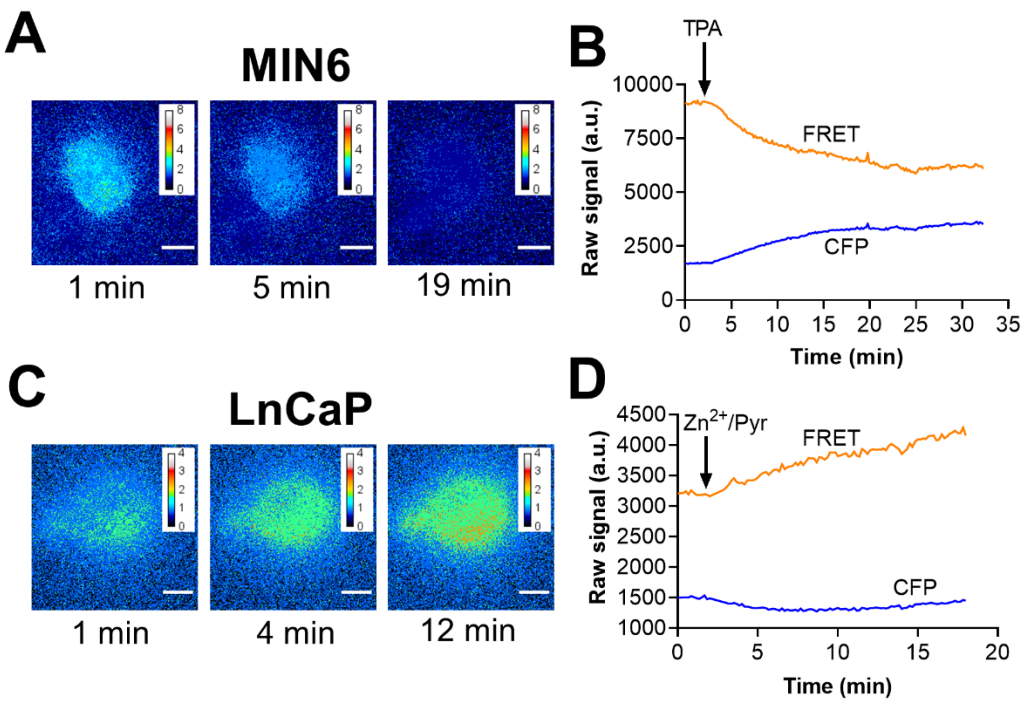

Figure S-11: FRET ratio images and reciprocal FRET and CFP traces from wide field Zn^{2+} calibrations in MIN6 cells and LnCaP cells expressing CgA-ZapCY1. (A&C) Representative FRET ratio images of a MIN6 cell (A) and LnCaP cell (C) expressing CgA-ZapCY1 at three different stages of a Zn^{2+} calibration on the wide field microscope. Three images are shown for each cell type: before the addition of TPA or Zn^{2+} (1 min), within 4-5 min after the addition of TPA or Zn^{2+} and once the FRET ratio had stabilized (12 min or 19 min for MIN6 and LnCaP, respectively). Images are shown in pseudocolor. Scale bar = 10 μm. (B&D) Reciprocal FRET and CFP traces that correspond with the images on the left.

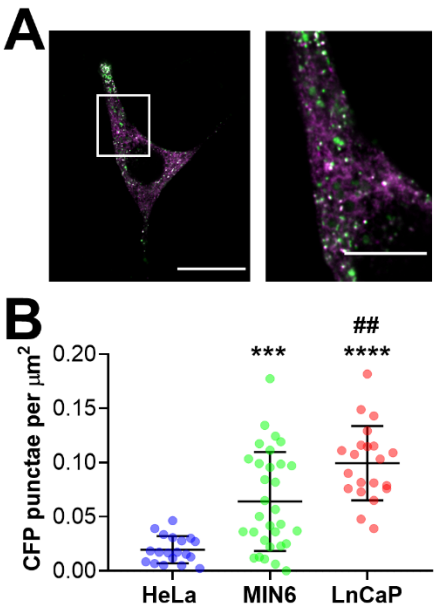

Figure S-12: CgA-ZapCY1 accumulates in vesicular puncta in LnCaP cells. (A) Representative image of a LnCaP cell expressing CgA-ZapCY1 that was collected using a spinning disk confocal microscope. The image on the left is an overlay of the CFP channel (green) and YFP channel (magenta). Scale bar = 25 µm. The image on the right is a magnified view of the selected region (white box). Scale bar = 10 µm. (B) Dot plot of CFP puncta detected per cell in HeLa, MIN6 and LnCaP cells, normalized to cell area (μm^2). Three independent experiments were performed per cell line and the average ± standard deviation is shown for n=19 cells (HeLa), n=31 cells (MIN6) and n=21 cells (LnCaP). Statistical analysis was performed using a One-Way ANOVA test with *post hoc* Tukey (****, $P < 0.0001$, ***, $P < 0.001$ compared with HeLa; ##, $P < 0.01$ compared with MIN6).

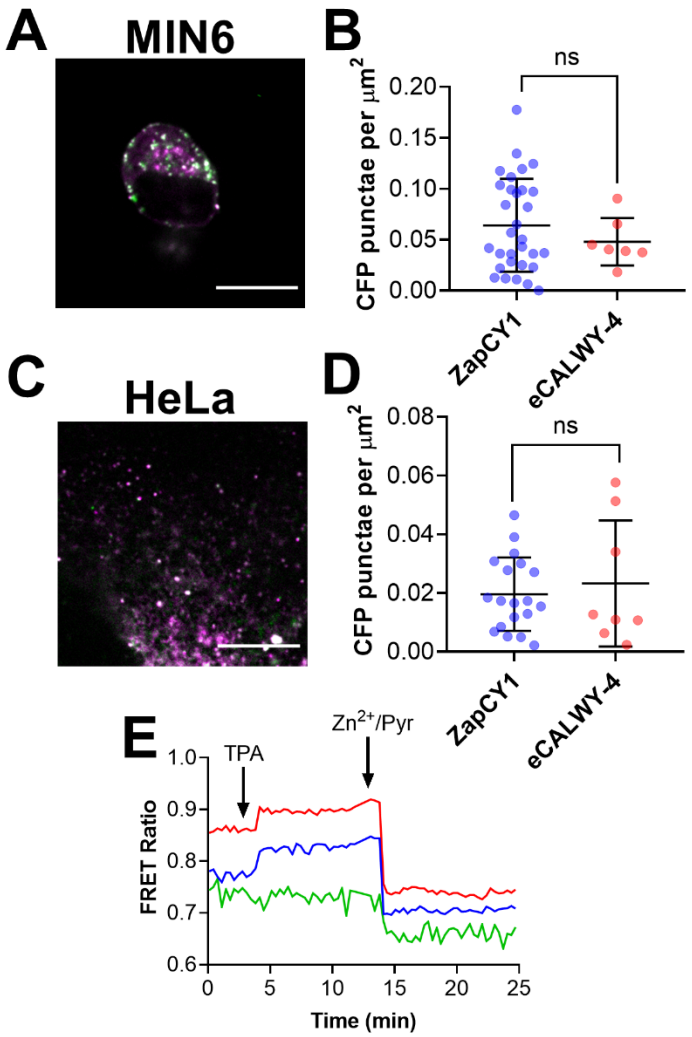

Figure S-13: CgA-eCALWY-4 accumulates in vesicular puncta in MIN6 cells and HeLa cells and responds to Zn^{2+} perturbations in MIN6 cells. (A&C) Representative image of a MIN6 cell (A) and HeLa cell (C) expressing CgA-eCALWY-4 that were collected using a spinning disk confocal microscope. The images shown are an overlay of the CFP channel (green) and YFP channel (magenta). Scale bar = 10 μm. (B&D) Dot plot of CFP puncta detected per MIN6 cell (B) and HeLa cell (D). There was no statistical difference (ns = not significant) between CgA-ZapCY1 and CgA-eCALWY-4 in MIN6 cells (B) or HeLa cells (D). (E) Time-lapse of the FRET ratio in three MIN6 cells expressing CgA-eCALWY-4 during a Zn^{2+} calibration on the wide field microscope.

Video S-1: Vesicular localization and dynamics in HeLa cell expressing CgA-ZapCY1. This video was captured using a spinning disk confocal microscope. Scale bar = 10 μm.

Video S-2: Vesicular localization and dynamics in MIN6 cell expressing CgA-ZapCY1. This video was captured using a spinning disk confocal microscope. Scale bar = 10 μm.

Video S-3: Vesicular localization and dynamics in LnCaP cell expressing CgA-ZapCY1. This video was captured using a spinning disk confocal microscope. Scale bar = 10 μm.

	Targeting signals derived from vesicular proteins
VAMP2 (Rat)	MSATAATVPPAAPAGEGGPPAPPPNLTSNRRLQQTQAQVDEVVDIMRVNVDKV LERDQKLSELDDRADALQAGASQFETSAAKLKRKYWWKNLKMMIILGVICAIILIII VYFSTSDPM
Syp (Rat)	MDVVNQLVAGGQFRVVKEPLGFVKVLQWVFAIFAFATCGSYTGELRLSVECAN KTESALNIEVEFEYPFRLHQVYFDAPSCVKGGTTKIFLVGDYSSSAEFFVTVAVF AFLYSMGALATYIFLQNKYRENNKGPMMDFLATAVFAFMWLVSSSAWAKGLSD VKMATDPENIIKEMPLCRQTGNTCKELRDPVTSGLNTSVVFGFLNLVLWVGNLW FVFKETGWAAPFMRAPPGAPEKQPAPGDAYGDAGYGQGPGGYGPQDSYGPQ GGYQPDYGQPASGGGGYGPQGDYGQQGYGQQGAPTSFSNQMGTELGSM
CgA (Human)	MRSAAVLALLLCAGQVTALPVNSPMNKGDTEVMKCIVEVISDTLSKPSPMPVSQ ECFETLRGDERILSILRHQNLLKELQDLALQGAKERAHQQKKHSGFEDELSEVLE NQSSQAELKEAVEEPSSKDVMEKREDSKEAEKSGEATDGARPQALPEPMQES KAEGNNQAPGEEEEEEEEATNTHPPASLPSQKYPGPQAEGDSEGLSQGLVDR EKGLSAEPGWQAKREEEEEEEEEAEAGEEAVPEEEGPTVVLNPHPSLGYKEIR KGESRSEALAVDGAGKPGAEEAQDPEGKGEQEHSQQKEEEEEMAVVPQGLFR GGKSGELEQEEERLSKEWEDSKRWSKMDQLAKELTAEKRLEGQEEEEDNRDS SMKLSFRARAYGFRGPGPQLRRGWRPSSWEDSLEAGLPLQVRGYPEEKKEEE GSANRRPEDQELESLSAIDAELEKVAHQLQALRRGSDPM
NPY (Human)	MLGNKRLGLSGLTLALSLLVCLGALAEAYPSKPDNPGEDAPAEDMARYYSALRH YINLITRQRYGKRSSPETLISDLLMRESTENVPRTRLEDPAMWKLM
INS (Mouse)	MALWMRFLPLLALLFLWESHPTQAFVKQHLCGSHLVEALYLVCGERGFFYTPM SRRM...KKRGIVDQCCTSICSLYQLENYCN

Table S-1: Amino acid sequences of targeting motifs used in this study. The targeting motif (black), linker sequence (blue) and first amino acid (and last amino acid in INS-mCherry) of the fluorescent sensors (red) used in this study are shown.

EDTA	**0.1**	**0.2**	**0.3**	**0.4**	**0.5**	**0.6**	**0.7**	**0.8**	**0.9**
pH 7.4	0.00327	0.00735	0.0126	0.0196	0.0294	0.0441	0.0686	0.118	0.264
pH 6.5	0.0371	0.0834	0.143	0.222	0.334	0.5	0.778	1.33	3

HEDTA	**0.1**	**0.2**	**0.3**	**0.4**	**0.5**	**0.6**	**0.7**	**0.8**	**0.9**
pH 7.4	0.0938	0.211	0.362	0.563	0.844	1.27	1.97	3.38	7.6
pH 6.5	0.804	1.81	3.1	4.83	7.24	10.9	16.9	29	65.2
pH 5.5	14.4	32.3	55.4	86.1	129	194	301	517	1163

HEDTA/Sr^{2+}	**0.1**	**0.2**	**0.3**	**0.4**	**0.5**	**0.6**	**0.7**	**0.8**	**0.9**
pH 7.4	1.94	4.76	8.83	14.8	23.8	38	62.9	114	271
pH 6.5	1.94	4.76	8.83	14.8	23.8	38	62.9	114	271

HEDTA/Ca^{2+}	**0.1**	**0.2**	**0.3**	**0.4**	**0.5**	**0.6**	**0.7**	**0.8**	**0.9**
pH 7.4	48.7	119	222	372	597	955	1579	2866	6807
pH 6.5	48.7	119	222	372	597	955	1579	2866	6807

EGTA	**0.1**	**0.2**	**0.3**	**0.4**	**0.5**	**0.6**	**0.7**	**0.8**	**0.9**
pH 7.4	0.115	0.258	0.443	0.688	1.03	1.55	2.41	4.13	9.29
pH 6.5	7.04	15.8	27.2	42.2	63.4	95	148	253	570
pH 5.5	701	1578	2705	4208	6312	9468	14728	25249	56809

Table S-2: Buffered Zn^{2+} solutions. Total Zn^{2+} concentrations (top row) are shown in mM. Free Zn^{2+} concentrations (bottom 2-3 rows) are shown in pM, except EGTA which is shown in nM.

Supporting Methods

Materials. *Preparation of stocks for Zn^{2+} titrations.* The Zn^{2+} chelator tris(2-pyridylmethyl)amine (TPA), Zn^{2+} ionophore 2-mercaptopyridine N-oxide (pyrithione), $ZnCl_2$ and saponin were purchased from Sigma-Aldrich. A 20 mM stock of TPA was prepared in DMSO and diluted to a 2x concentration (100 µM or 300 µM) for experiments. A 5 mM stock of pyrithione was prepared in DMSO and diluted to a 2x concentration (10 µM) for experiments. A 10 mM stock of $ZnCl_2$ was prepared in chelex-treated dH_2O and diluted to a 2x concentration (20 µM) for experiments. A 0.1% stock of saponin was prepared in chelex-treated dH_2O and diluted to a 2x concentration (0.002%) for experiments. TPA was diluted in phosphate-free HEPES-buffered Hanks Buffered Salt Solution (HHBSS) adjusted to pH 7.4: 137 mM NaCl, 5.4 mM KCl, 1.26 mM $CaCl_2$, 1.1 mM $MgCl_2$, 20 mM HEPES, 3 g/L glucose and 0.35 g/L $NaHCO_3$. Pyrithione, $ZnCl_2$ and saponin were diluted in phosphate-, calcium- and magnesium-free HHBSS adjusted to pH 7.4: 137 mM NaCl, 5.4 mM KCl, 20 mM HEPES, 3 g/L glucose and 0.35 g/L $NaHCO_3$ at pH 7.4

Preparation of stocks for pH calibration and titrations. A 20 mM solution of NH_4Cl (Sigma-Aldrich) was prepared in chelex-treated dH_2O and adjusted to pH 8.5. A 50 mM stock of monensin sodium salt (Fluka) was prepared in ethanol and diluted to a final concentration of 10 µM for experiments. A 5 mM stock of nigericin sodium salt (Sigma-Aldrich) was prepared in ethanol and diluted to a final concentration of 10 µM for experiments. A 5 mM stock of digitonin (Calbiochem) was prepared in DMSO and diluted to a final concentration of 10 µM for experiments. Final concentrations of monensin, nigericin and digitonin were prepared in pH clamp buffers (pH 3.5-7.5): 125 mM KCl, 25 mM NaCl and 25 mM HEPES (pH 7-7.5) or 25 mM MES (pH 3.5-6.5).

Molecular cloning. *Vesicular mCherry and Zn^{2+} FRET sensors:* Targeting signals derived from vesicular proteins were inserted upstream of mCherry (VAMP2, Syp, CgA, NPY, INS) and ZapCY1 (VAMP2, CgA, NPY). The amino acid sequences of the targeting signals are shown in Table S-1. The vector backbone for all constructs was pcDNA3, unless otherwise indicated. To make Syp-mCherry, Syp-GZnP was digested with BamHI and XhoI to remove GZnP. mCherry was PCR amplified from VAMP2-mCherry and inserted downstream of Syp. To make INS-mCherry (pLX304), Proinsulin-NanoLuc (Addgene Plasmid #62057) was linearized by PCR, removing the C-peptide and NanoLuc. mCherry was PCR amplified from VAMP2-mCherry and inserted in between the B- and A-chain of proinsulin [52]. To make NPY-mCherry and NPY-ZapCY1 [53], NPY-pHluorin (gift from Gregory Hockerman at Purdue University) was digested with HindIII and EcoRI to remove pHluorin. mCherry and ZapCY1 were PCR amplified from VAMP2-mCherry and VAMP2-ZapCY1, respectively, and inserted downstream of NPY. To make VAMP2-ZapCY1, NES-ZapCY1was digested with KpnI and BamHI to remove the NES. VAMP2 was PCR amplified from VAMP2-ZapmNGmR1 and inserted upstream of ZapCY1. To make CgA-ZapCY1, VAMP2-ZapCY1 was digested with KpnI and BamHI to remove VAMP2. CgA was PCR amplified from CgA-mCherry and inserted upstream of ZapCY1.

To make CgA-eCALWY4, CgA was amplified by PCR with a 5' EcoR1 site from the pcDNA-CgA-mScarlet-1 plasmid and was inserted before eCALWY-4 in the peCALWY-4 plasmid (Addgene Plasmid #22236) using Gibson assembly.

Colocalization markers. The mCherry organelle markers used in colocalization analysis included Sec61β-mCherry (mCherry-N1), GalT-mCherry, mCherry-Rab5a, Rab7-mCherry (mCherry-N1) and pLAMP1-mCherry (Addgene Plasmid #45147). VAMP2-mCherry, NPY-mCherry and INS-mCherry (described above) were also used as organelle markers.

Cell culture and transfection. HeLa cells (ATCC CLL-2) were cultured in DMEM (Invitrogen) containing 10% fetal bovine serum (FBS) and 1% Penicillin-Streptomycin (P/S). For HeLa cell transfections, 1 µg total DNA and 3 µL TransIT-LT1 (Mirus Bio) were added to 200 µL OPTI-

MEM (Thermo Fisher Scientific) and the mixture was incubated at room temperature for 5 minutes. The transfection mixture was added drop-wise to HeLa cells plated in custom-made imaging dishes. For colocalization experiments in HeLa cells, 500 ng CgA-Zn^{2+} FRET sensor and 500 ng mCherry organelle markers were used. MIN6 cells (AddexBio) were cultured in AddexBio Optimized DMEM containing 15% FBS, 1% P/S and 50 μM cell culture-grade β-mercaptoethanol. LnCaP cells were cultured in RPMI-1640 (Gibco) containing 10% FBS and 1% P/S. For MIN6 and LnCaP cell transfections, 2.5 μg total DNA and 7.5 μL Lipofectamine 2000 (Thermo Fisher Scientific) were added to 200 μL OPTI-MEM and the mixture was incubated at room temperature for 15 minutes before adding drop-wise to cells plated in 6-well dishes. For colocalization experiments in MIN6 cells, 1.25 μg CgA-Zn^{2+} FRET sensor and 1.25 μg mCherry organelle markers were used. At 24 hours post-transfection, MIN6 and LnCaP cells were transferred to 8-chamber IbiTreat-treated μ-Slide 8 Well plates (Ibidi). All cell lines were cultured at 37˚C and 5% CO_2 and imaged at 48 hours post-transfection under the same conditions. The passage numbers of the cell lines used in this study were: passage 9-18 (HeLa), passage 17-26 (MIN6) and passage 15-21 (LnCaP).

Fluorescence Microscopes. A Nikon spinning disk confocal microscope equipped with a Ti-E perfect focus system, CSU-X1 spinning disc head (Yokogawa), 888 Ultra EMCCD camera (Andor) and Plan Apo λ 100x oil objective lens (NA 1.45) was used for most imaging experiments. The following laser lines and emission filters were used: 445 nm laser and 482/35 nm emission filter (CFP), 515 nm laser and 540/30 nm emission filter (YFP), 445 nm laser and 540/30 nm emission filter (FRET), 594 nm laser and 630/30 nm emission filter (mCherry). The readout speed (10 MHz) and EM multiplier (300) was consistent across all experiments. The laser power, binning and exposure varied (see below).

A Nikon wide field fluorescence microscope equipped with a Ti-E perfect focus system, iXon3 EMCCD camera (Andor), mercury arc lamp, lambda 10-3 filter changer (Sutter Instruments) and Plan Apo VC 60x DIC N3 oil objective lens (NA 1.4) was used in some experiments. For the CFP channel, a 434/16 nm excitation filter, 458 dichroic and 470/24 nm emission filter were used. For the YFP channel, a 494/10 nm excitation filter, 515 dichroic and 510/10 nm emission filter were used. For the FRET channel, a 434/16 nm excitation filter, 458 dichroic and 535/20 emission filter were used. For the mCherry channel, a 560/20 nm excitation filter, 585 dichroic and 610/50 nm emission filter were used. The readout speed (1 MHz at 16-bit readout mode), EM multiplier (300) and use of an ND4 filter was consistent across experiments. The exposure varied (50-200 ms).